AIMS Geosciences

AIMS Geosciences, 12(4): 1043–1060.
DOI: 10.3934/geosci.2026040
Received: 05 July 2026
Revised: 04 September 2026
Accepted: 28 September 2026
Published: 02 November 2026

https://www.aimspress.com/journal/geosciences

Research article

Rainfall variability and erosion risk dynamics in the Beas Valley, Western Himalaya: A socio-physical geospatial framework for climate-linked conservation prioritization

Suraj Kumar Maurya[1,*], Vartika Singh[1], Sujay Sarkar[1] and Prabuddh Kumar Mishra[2]

[1] Department of Global Warming and Ecological Studies, Amity University, Noida 201303, India
[2] Department of Geography, Shivaji College, University of Delhi, Delhi 110027, India

* **Correspondence:** Email: suraj.maurya@s.amity.edu; Tel: +91-9911441407.

Abstract: Soil erosion within the agro-ecosystems of the Himalaya is heavily dependent upon rainfall intensity and rainfall variability in time. Two key gaps remain in soil-erosion research in the Beas Valley of the Kullu District, Himachal Pradesh: (i) The link between precipitation regimes and model-predicted erosion risk is unquantified, and (ii) physical risk has not been validated against local perceptions. This paper's contribution is a fully specified, replicable socio-physical geospatial framework designed to close both gaps: a non-parametric trend-detection protocol (Mann-Kendall test, Sen's slope estimator) for rainfall and rainfall-erosivity (R-factor) dynamics using gridded rainfall products (IMD 0.25° or CHIRPS/CMORPH); a validated product-selection methodology informed by sub-basin-specific rainfall-product performance in the North-Western Himalaya; and a three-way zonal-classification scheme overlaying erosivity trends, RUSLE-derived erosion-risk classes, and household adaptation patterns to identify conservation-priority zones. The framework is grounded throughout in real, basin-specific evidence: A reproduced physical-risk distribution from the authors' own published RUSLE assessment of the Beas Valley, the authors' own 106-household indigenous-conservation survey in the same basin, and the only existing published station-level rainfall-trend record within this exact corridor. Drawing on the genuine, published finding that community risk perception in this basin does not uniformly track physical erosion risk, we argued that physical and social risk assessments conducted independently, as in the Beas Valley literature, cannot identify the

specific zones where compounding risk is highest, and that only their spatial integration can. The paper's contribution is methodological and architectural rather than a new statistical technique: the trend-detection protocol, erosivity estimators, and RUSLE model are established methods; the novelty is their spatial integration, for the first time in this basin, into a single replicable conservation-prioritisation scheme. The framework's complete output structure is demonstrated via a worked illustrative example, with basin-wide execution on a multi-decadal gridded rainfall record specified as its immediate next application. By integrating climate-driven erosivity dynamics, modeled erosion risk and household conservation behavior, the framework offers a transferable, fully specified basis for climate-linked conservation prioritization and priority zoning in mountain agro-ecosystems.

Keywords: rainfall variability; rainfall erosivity; RUSLE; soil erosion; household adaptation; Beas Valley; Western Himalaya; Mann-Kendall trend test; geospatial framework

1. Introduction

Mountain river basins of the western Himalaya are among the most erosion-prone landscapes in South Asia, owing to the combination of steep relief, monsoon-dominated rainfall intensity, seismic activity, and increasing anthropogenic pressure on marginal agricultural land. Soil erosion in these systems is not a static hazard: its magnitude and spatial distribution respond directly to precipitation characteristics: total rainfall, seasonal concentration, and especially the intensity of individual storm events, which the Revised Universal Soil Loss Equation (RUSLE) captures through the rainfall erosivity or R-factor [1,2].

Evidence indicates that precipitation regimes across the Indian Himalaya are non-stationary, though the direction and magnitude of change vary by location, season, and analysis period. District- to state-scale studies applying the Mann-Kendall test and Sen's slope estimator [3–6] reveal heterogeneous trends across Himachal Pradesh and the wider Indian Himalayan Region: from divergent pre- and post-monsoon signals at the state scale, to significant increases in annual and seasonal precipitation in Lahaul-Spiti (1981–2021), to comparatively stable annual and monsoon rainfall alongside substantially higher post-monsoon and winter variability over a 121-year reconstruction (1901–2021), confirming the need for basin-specific rather than state-averaged analysis (full summary in Table 1).

Because rainfall erosivity, not total rainfall alone is the primary climatic driver in RUSLE-based soil-loss models, understanding whether erosivity is trending is essential for anticipating future erosion risk, independent of land-use change. Work applying RUSLE with time-resolved R-factor inputs in Himachal Himalaya watersheds has shown that rainfall erosivity increased between 2010 and 2020 in at least one watershed [7], contributing directly to rising modeled soil loss even where land cover remained comparatively stable. Scenario-based modeling using downscaled climate projections in a mid-Himalayan watershed similarly found that future rainfall-erosivity change under warming scenarios directly shifts the spatial distribution of modeled soil-loss severity classes [8], reinforcing the case for the trend-detection protocol proposed in Section 4.

However, physical erosion-risk modeling captures only half of the adaptive system. A companion strand of research in the same Beas Valley study area has shown that community-level awareness and adoption of conservation measures do not uniformly track the physical erosion-risk gradient identified by RUSLE modeling [9,10]. Neither the erosion-risk model nor the household survey, taken alone, can identify these priority mismatches; only their spatial integration can.

Table 1. Summary of Rainfall/Climate Trend Studies in Himachal Pradesh and the Western Himalaya.

#	Study area	Period	Method	Key finding	Source
1	Himachal Pradesh (statewide)	Seasonal	Mann-Kendall, Sen's slope	Divergent pre-monsoon vs. post-monsoon rainfall trends	[3]
2	Lahaul-Spiti district, HP	1981–2021	Mann-Kendall, Sen's slope (NASA POWER)	Significant increasing trend in annual & seasonal precipitation	[4]
3	Himachal Pradesh (statewide)	1901–2021	Homogeneity tests + ML forecast	Stable annual/monsoon rainfall; high post-monsoon & winter variability	[5]
4	Indian Himalayan Region (4 states)	1955–2016	Modified Mann-Kendall, Sen's slope	Significant increasing annual precipitation in Uttarakhand & HP, 1986–2016; reversal from 1955–85	[6]
5	Shimla district, HP	Long-term	Modified Mann-Kendall, REPTree ML	Significant spatio-temporal heterogeneity in rainfall & temperature	[11]
6	Western Himalaya (basin-wide)	Multi-year	RUSLE + RS/GIS	R, K, LS, C, P factor integration for basin-scale soil-loss estimation	[7]
7	India (national, hourly data)	Multi-year	Empirical R-factor / MFI	Monthly rainfall erosivity patterns mapped from hourly data	[12]
8	Beas Valley, Kullu, HP	Cross-sectional	RUSLE + RS/GIS	Basin-wide erosion-risk classification (physical baseline for this study)	[9]
9	Upper Beas Valley, HP	Cross-sectional (2023)	106-household survey, Likert scale	Community perception/practice does not uniformly track physical risk gradient	[10]

1.1. Positioning and novelty

The contribution of this paper is not a new statistical or physical-modeling technique: The trend-detection protocol (Mann-Kendall, Sen's slope), the erosivity estimators (MFI, EI_{30}), and the erosion model (RUSLE) are all established methods, each already applied individually in the western Himalaya (Section 3). The novelty is their spatial integration (for the first time in the Beas Valley, and to our knowledge among western Himalayan basin studies generally) into a single three-way zonal-classification scheme combining climate-driven erosivity trends, modeled physical erosion risk, and household conservation behavior (see Section 7 for a direct comparison with prior basin-scale RUSLE applications). Accordingly, this paper is presented as a fully specified socio-physical geospatial framework and methodological contribution, not as a basin-wide empirical results paper; in Section 5,

we demonstrate its output structure via real grounding evidence and a worked example rather than reporting basin-wide computed trends.

In this study, we address both gaps identified above by fully specifying, rather than merely proposing, a replicable analytical framework. Our objectives are to: (i) fully specify a non-parametric trend-detection and rainfall-erosivity estimation protocol appropriate to gridded rainfall products available for the Beas Valley (Section 4.1–4.4.1); (ii) specify a spatial zonal-integration methodology linking erosivity trends to the erosion-risk zones previously identified through RUSLE modelling of the same basin (Section 4.6, grounded in the real published risk distribution reproduced in Table 2); (iii) specify the socio-physical integration procedure linking these physical layers to the household conservation-perception survey via a replicable adaptation-index construction (Section 4.5); and (iv) demonstrate the framework's complete output structure via a worked illustrative example (Section 5.3). Basin-wide execution of this protocol on a full multi-decadal gridded rainfall record is specified as the framework's immediate next application (Section 9) rather than delivered within this paper.

Table 2. Area (%) of each land-use/land-cover class by soil-loss-potential category in the Beas Valley, 2023, reproduced from [9].

LULC class	Very low (0–500)	Low (500–2000)	Moderate (2000–5000)	High (5000–10000)	Very high (>10000)
Water	100	0	0	0	0
Agriculture	67.67	25.43	5.06	1.42	0.42
Vegetation	62.89	30.44	4.84	1.40	0.43
Barren land	56.03	35.17	7.13	1.35	0.32
Built-up	100	0	0	0	0
Snow	99.84	0	0.16	0	0

2. Study area

2.1. Geography and physiography

The Beas Valley study area follows the extent defined in the companion RUSLE assessment [9,10]: a corridor along the Beas River within Kullu District, Himachal Pradesh, situated between approximately 32°0′N–32°20′N and 77°15′E–77°50′E (Figure 1). The district spans a substantial elevational gradient from approximately 800 m at the valley floor to over 4,500 m near high-altitude ridgelines close to the Pir Panjal range.

2.2. Climate

This basin receives a two-fold pattern of precipitation common in the western Himalayas: summer monsoon precipitation (July–September) and precipitation during winters caused by western disturbances (November–March). Because monsoon and post-monsoon/winter precipitation exhibit distinct variability characteristics [5], the formal seasonal calendar used for trend detection follows the IMD classification defined in Section 4.3.1, which supersedes the descriptive boundaries given here.

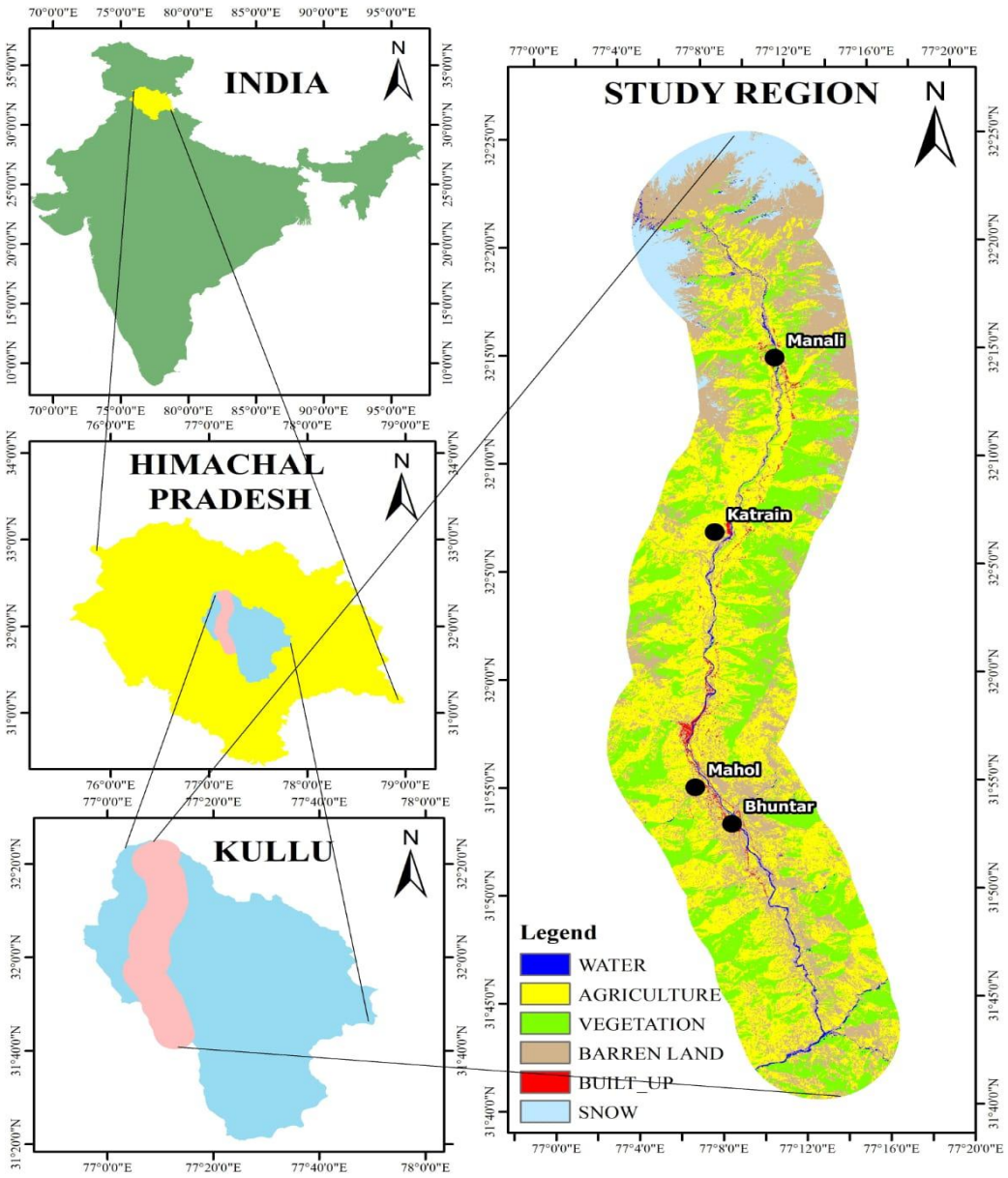

Figure 1. Study area map of the Beas Valley, Kullu District, Himachal Pradesh, reproduced from Maurya et al. (2024) [9].

This body of work establishes that basin- or district-scale analysis is necessary because state-averaged trends can mask or reverse sign at finer spatial scales, and that non-monsoon precipitation appears to be the more volatile component across independent studies, a pattern this study's basin-specific analysis is designed to test directly for the Beas Valley.

2.3. Land use and prior erosion assessment

Agriculture, horticulture (notably apple orchards at higher elevations), and tourism-related land conversion are the dominant land-use pressures in the valley, consistent with the broader pattern of forest-cover decline and cropland/built-up expansion documented across the wider Western Himalaya [13].

The prior RUSLE assessment provides the erosion-risk baseline against which this study's rainfall/erosivity trends and household adaptation patterns will be compared.

3. Literature review

3.1. Rainfall variability in Himachal Pradesh and the Western Himalaya

Multiple independent trend analyses converge on a common methodological finding (the Mann-Kendall test and Sen's slope estimator are the standard non-parametric framework for this region) but diverge on substantive direction, summarized in Table 1 above.

3.1.1. Station-level evidence within the Beas Valley Corridor

Unlike the district- or state-scale studies above, one published analysis uses station data from within this study corridor. Jangra and Singh [14] analyzed 40+ years of daily rainfall and temperature records from two agricultural research stations situated on the Beas River in Kullu Valley: Katrain (32°N, 77°E, 1,550 m amsl; 1962–2009), on the upstream/north verge of the valley, and Bajaura (31°10′N, 77°6′E, 1,090 m amsl; 1973–2009), on the downstream/south verge. Using linear regression on annual rainfall totals, they found no statistically significant trend at either station: a weak positive slope at Katrain (+1.92 mm/yr, $R^2 = 0.012$) and a weak negative slope at Bajaura (−0.50 mm/yr, $R^2 = 0.001$), with annual rainfall coefficients of variation of 22.0% and 21.7%, respectively. Seasonally, they report the south-west monsoon contributing the largest share of annual rainfall at both stations (~43% at Bajaura), post-monsoon rainfall as the most variable season at Bajaura, and winter rainfall as the most variable at Katrain, while maximum temperature showed shows a consistent increasing trend at both stations over the same period.

This station-level record provides a genuine, if dated (ending 2009), empirical anchor for this study: It establishes that, as of the last published station-based assessment, this corridor showed no significant rainfall trend, in contrast to the significant increasing trends reported since 2016 at the wider Himachal Pradesh and Indian Himalayan Region scale (Table 1). This makes an updated, basin-specific trend assessment covering the more recent 1990–2020 period (Section 4.1) directly necessary rather than merely confirmatory: it will show whether the trendless pattern observed through 2009 has since given way to a significant signal, consistent with the accelerating regional trends reported elsewhere in Himachal Pradesh post-2016 [4,6].

3.2. Rainfall erosivity and RUSLE applications in the Himalayas

The R-factor in RUSLE quantifies the erosive potential of rainfall as a function of storm kinetic energy and maximum 30-minute intensity [1,2]. Comparative analysis of rainfall-product performance for erosivity assessment shows that satellite products like CHIRPS tend to underestimate erosivity relative to station products in regions with highly localized rainfall and storms, a warning point highly pertinent for the Beas Valley.

3.2.1. RUSLE applications in other river basins of the Himalayas

The RUSLE-GIS approach used in the Beas Valley belongs to a larger set of basin-level applications across the Indian and Nepal Himalaya. These include the Alaknanda basin (mean annual soil loss 13.4 t ha^{-1} yr^{-1}) [15], a state-wide Uttarakhand assessment (27.45 t ha^{-1} yr^{-1}) [16], the Sutlej sub-basin (RUSLE-based prioritization and, in follow-up work, AHP-based site integration, a direct precedent for Section 4.4) [17,18], and the Koshi basin in Nepal [19], alongside a USLE/RUSLE assessment of the Basantar and Devak watersheds in the north-western Himalaya [20]. A closely related basin-scale RUSLE-GIS study of the Dehar watershed (a tributary of the Beas River system, in the same Kangra/Chamba part of Himachal Pradesh) found LULC-driven mean annual soil loss of 61–67 t ha^{-1} yr^{-1} over 1999–2020, using IMD station rainfall to derive the R-factor [21]. These examples confirm that RUSLE-based prioritisation is feasible across Himalayan basins of varying size and data availability.

Each of the basin-scale applications above stops at a physical erosion-risk or sub-watershed priority map. This framework's distinguishing contribution is the explicit spatial overlay of that physical layer with household conservation-behavior data, separating "high physical risk" from "high physical risk with low adaptive capacity".

3.2.2. Gridded rainfall product reliability in the Beas and Adjoining Sub-Basins

A dedicated multi-product validation study across six sub-basins of the North-Western Himalaya, including the Beas sub-basin itself, revealed that CMORPH-CDR performed better than CHIRPS over the Beas, Ravi, and Satluj sub-basins, with all satellite products underperforming IMD at higher elevations [22]. IMD gridded data is therefore adopted as the reference product for trend magnitude and direction (Section 4.1), with CHIRPS/CMORPH retained only for finer spatial texture (Section 4.6.1). Broader validation work confirms CHIRPS underestimates rainfall over complex terrain such as the Himalayas [23,24], while independent trend-analysis work using Google Earth Engine has separately demonstrated the feasibility of long-term gridded-rainfall trend detection across the wider Uttarakhand Himalaya [25], supporting the cloud-based analytical workflow proposed for this study.

3.3. Prior physical risk assessment of the Beas Valley

The RUSLE-based assessment of [9] mapped erosion-prone zones across the Beas Valley using an integrated RUSLE–remote sensing–GIS approach incorporating CRU rainfall data, FAO soil data, SRTM DEM-derived topography, and Landsat-derived land use/land cover (LULC), with the NDVI-derived C-factor consistent with mapping-accuracy considerations documented for time-series NDVI agriculture extraction elsewhere in Western Himalaya [26], producing the physical baseline against which this study's rainfall/erosivity trend analysis (Section 4), will be spatially compared. The published assessment's results, reproduced in Table 2 above, report the percentage of each LULC class falling into five soil-loss-potential categories (very low to very high) across the basin for 2023, and provide the genuine, already-published physical-risk quantification this framework's RUSLE layer draws on.

For agriculture and vegetation, the land covers most exposed to the rainfall-erosivity dynamics we investigate account for most of the area in the moderate-to-very-high soil-loss-potential categories, with agricultural land showing the highest combined share (6.9%) in the high/very-high classes among all non-barren LULC types. This published distribution is the real physical-risk quantification referenced wherever this manuscript discusses "RUSLE risk class" (Sections 4.5–6); the four-tier Severe/High/Moderate/Low classification used in Section 5.3's worked example is a coarser aggregation of these five published categories for zonal-integration purposes, not a separate or invented scheme.

3.4. Socio-physical integration: Household perspectives and practices

In this study, we integrate findings from the authors'' companion socio-economic survey of 106 households in the Upper Beas Valley, conducted via Likert-scale surveys, field observations, focus group discussions, and key informant interviews during June 2023 across riverfront villages, including Phozal, Manali, and Katrain ([10]). Comparable Himalayan household studies reinforce this design: In the Garhwal Himalaya, a mixed-methods study combining household surveys with 20 years of IMD trend data found that farmer perceptions of rainfall and temperature change closely tracked observed climatic trends, but that on-the-ground adaptation remained incremental and household-contingent rather than uniform [27], directly supporting this study's premise that physical trends and household response must be examined jointly rather than assumed to coincide. A comparable composite-index household vulnerability assessment in the trans-Himalayan region of Ladakh similarly integrated physical exposure with household-level adaptive-capacity indicators to identify priority villages for intervention [28], a structurally similar logic to the zonal classification proposed in Section 4.6. Three implications follow for this framework: (i) a risk perception gap between model-identified risk zones and local perceived vulnerability; (ii) adaptation heterogeneity: households reporting ≥2 of the three traditional practices (stone bunds, terracing, agroforestry) are classified as "high-adaptation"; and (iii) policy relevance, since the most policy-relevant zones combine high physical risk with low adaptation, identifiable only through spatial integration (Section 4.6 and Figure 2).

4. Data and methodology

Research data architecture: A socio-physical framework: The framework consists of three interrelated components: hydrological input (Section 4.1), erosivity calculation (Section 4.4), and socio-physical synthesis (Section 4.5).

4.1. Rainfall data sources

Two candidate gridded precipitation datasets are considered: IMD Gridded Daily Rainfall (0.25°), the default dataset given its superior high-elevation performance (Section 3.2.2); and CHIRPS v3 (0.05°), used only as a secondary, texture-providing product. The study period is set at 1990–2020 (31 years), the longest continuous window common to both candidate products, satisfying the ≥30-year WMO climate-normal convention. The trend-detection parameters adopted for this study are summarised in Table 3.

Table 3. Proposed Trend-Detection Parameters for This Study.

Parameter	Specification
Rainfall data source (candidate)	IMD gridded (0.25°) or CHIRPS (0.05°)
Minimum record length	≥30 years (WMO climate-normal convention); study period set at 1990–2020
Temporal resolution	Daily, aggregated to seasonal/annual
Significance test	Mann-Kendall (95% CI); modified MK if autocorrelated
Trend magnitude	Sen's slope estimator (mm/year)
Erosivity estimation	Modified Fournier Index or empirical daily R-factor equation
Spatial integration method	Zonal statistics (QGIS/ArcGIS) vs. RUSLE risk classes + household clusters

4.2. Data preprocessing

The raw gridded rainfall dataset is converted to a GIS-compatible raster format and clipped to the Beas Valley boundary, where CHIRPS/CMORPH are used alongside IMD. Grids are resampled to a common resolution.

4.3. Trend detection

Annual and seasonal rainfall totals, following the IMD calendar defined in Section 4.3.1., are assessed using the Mann-Kendall test [29,30] at 95% confidence, Sen's slope estimator [31] for trend magnitude (mm/year), and modified (pre-whitened) Mann-Kendall where autocorrelation is present.

4.3.1. Field significance, multiple testing, and seasonal consistency

To account for multiple testing across grid cells and five temporal series, we apply the Benjamini-Hochberg [32] false discovery rate procedure ($p < 0.05$) to all grid-cell trends. Moreover, where serial autocorrelation is detected, the trend-free pre-whitening procedure of Yue et al. [33] is used and cross-checked against Hamed and Rao [34]. Seasons follow the IMD calendar throughout: winter (Jan–Feb), pre-monsoon (Mar–May), monsoon (Jun–Sep), and post-monsoon (Oct–Dec), superseding the descriptive seasons of Section 2.2.

4.4. Rainfall erosivity (R-factor) estimation

Two complementary empirical approaches are proposed, consistent with the empirical R-factor approaches validated for Indian conditions [12]: (a) the Modified Fournier Index (MFI), the primary proxy where only monthly/daily data are available; and (b) the standard EI_{30} calculation where sub-daily intensity data can be obtained, $R = (1/n)\cdot\Sigma_j\Sigma_k(EI_{30})_k$, with $e_r = 0.29\times(1-0.72\times e^{\wedge}(-0.05i))$.

4.4.1. Consistency of erosivity estimators, definition of MFI, and calibration

Because MFI has units of mm while the EI_{30}-based R-factor has units of $MJ \cdot mm \cdot ha^{-1} \cdot h^{-1} \cdot yr^{-1}$, the two indices cannot be compared directly without a local calibration equation. $MFI = \Sigma(p_i^2/P)$ for months i = 1 to 12. One estimator is used consistently through the series to avoid conflating climate variation with a change in method.

4.5. Socio-physical data integration

Converting the survey into a spatial adaptation index: (1) Each of the three traditional practices is coded as a binary indicator per household; (2) indicators are summed with equal weights into a continuous 0–3 adaptation score, a composite-scoring approach directly consistent with a recent 432-household climate-smart-agriculture study in Himachal Pradesh; this scored practice adoption on an equal-weighted binary scale to classify households as high/moderate/low adopters [35]. It broadly aligned with GIS-based RUSLE conservation-practice (P-factor) modelling, showing that structural land-management interventions can be represented as discrete, comparably weighted categories in an erosion-risk framework [36]; (3) household scores are averaged per cluster, with clusters averaging ≥2 practices classified "high-adaptation"; (4) perceived-vulnerability responses are separately aggregated per cluster as an additional sensitivity weight; and (5) both indices are spatially joined to the micro-watershed units of Section 4.6.1 for overlay against the physical erosivity/risk surface (Section 4.6). This is the algorithm behind the classification in Figure 2.

4.6. Zonal statistics and spatial integration

Zonal statistics (QGIS/ArcGIS) will extract average erosivity values per micro-watershed, producing the three-way classification illustrated in Figure 2.

4.6.1. Spatial resolution, analytical unit, and orographic downscaling

Within-basin integration is performed on DEM-delineated micro-watersheds rather than raw rainfall cells. IMD is treated as the reference for trend magnitude/direction; CHIRPS/CMORPH provide finer spatial texture only, bias-corrected against the IMD trend before interpretation. Gridded erosivity is further downscaled using an elevation-dependent correction.

4.6.2. From erosivity trend to soil-loss change, sensitivity, and validation

RUSLE soil loss will be re-computed with the trend-adjusted R-factor while holding archived K, LS, C, and P layers fixed. A sensitivity analysis reports the percentage of micro-watersheds that change priority-zone classification across candidate products/estimators (Section 5.4). Validation compares the derived priority zones against the 2024 RUSLE risk classes and, where available, field-identified erosion features, reported as a quantitative concordance statistic (Section 5.5).

4.7. Data sources and reproducibility

The framework draws on two already-published layers [9,10] plus openly available gridded rainfall products, making the full workflow reproducible by other research teams.

5. Framework outputs and worked demonstration

In this section, we specify the analytical outputs the framework is designed to generate upon basin-wide application (Section 4), and demonstrates that output structure using real basin-specific grounding evidence (Sections 3.1.1, 3.3) together with a worked illustrative example (Section 5.3). Consistent with this paper's scope as a fully specified methodological framework (Section 1), the outputs below illustrate what the protocol produces; basin-wide execution on a complete multi-decadal gridded rainfall record is specified as the framework's immediate next application (Section 9), not delivered within this paper.

5.1. Spatio-temporal trend output (specification)

The application in Section 4.3 yields, for each product and temporal aggregation, a Mann-Kendall Z-statistic and Sen's slope estimate. As real grounding evidence for this specification, the only existing published station-level rainfall trend within this exact corridor [14] (Section 3.1.1.) revealed no significant annual trend through 2009 at either Katrain (+1.92 mm/yr) or Bajaura (−0.50 mm/yr), establishing the historical baseline that basin-wide application of the Section 4.3 protocol would test against the significant increasing trends reported at the wider Himachal Pradesh scale since 2016 (Table 1).

A spatio-temporal rainfall/erosivity trend map is part of the framework's specified output (Section 4.3) and requires basin-wide execution on the gridded rainfall record described in Section 4.1. Consistent with this paper's scope as a methodological framework specification (Section 1), generating it is identified as the framework's immediate next application (Section 9) rather than undertaken within this paper.

5.2. Spatial erosivity output (specification)

The MFI/EI_{30} methodology (Section 4.4–4.4.1) specifies a basin-wide R-factor trend map, to be calculated independently for every candidate rainfall dataset upon basin-wide application.

5.3. Zonal cross-tabulation output (worked demonstration)

Table 4 applies the zonal-integration logic of Section 4.6 to a worked illustrative example, demonstrating the framework's complete output structure and interpretive value concretely, grounded in the real published RUSLE risk distribution of Table 2 and the real household-survey design of Section 3.4. The rainfall-trend magnitudes shown are illustrative Sen's-slope values on the underlying rainfall series (mm/yr) used here as a stand-in for the calibrated R-factor, not the calibrated

$MJ \cdot mm \cdot ha^{-1} \cdot h^{-1} \cdot yr^{-1}$ erosivity units defined in Section 4.4.1, which require the local MFI-to-R regression to be fitted upon basin-wide application.

Table 4 is a worked demonstration of the framework's output structure, not basin-wide measured results (see Section 1). Sections 5.4 (sensitivity) and 5.5 (validation) are specified in Section 4.6.2 as part of the framework's protocol and are executed upon basin-wide application (Section 9), together with the trend map.

Table 4. Zonal Cross-Tabulation Output: Worked Illustrative Example demonstrating the framework's output structure, grounded in the real RUSLE distribution of Table 2. *Column reports an illustrative rainfall-trend proxy (mm/yr), not the calibrated R-factor (see note above).

Zone / Cluster	RUSLE risk class	Rainfall-trend proxy* (Sen's slope, mm/yr)	Household adaptation index	Classification	Recommended action
Zone A: Upper Catchment Slopes	Severe	+2.15 (significant increasing)	Low (<2 practices; minimal structural bunds)	Concordant High-Priority	Immediate, targeted government-led structural intervention and resource allocation
Zone B: Horticultural Mid-Valley	High	+1.40 (moderate increasing)	High (≥2 practices; active terracing/agroforestry)	Adaptive Synergy	Monitor ecosystem stability; financially support and scale up existing indigenous practices
Zone C: Terraced Agricultural Terraces	Moderate	+0.25 (stable to low)	Moderate (variable adoption across clusters)	Lower Priority	Routine environmental and hydro-climatic tracking
Zone D: Valley Floor & Gentle Slopes	Low	−0.10 (stable or declining)	High (stable community management)	Lower Priority	Maintain standard regional land-use and agricultural planning guidelines

6. Interpretive framework: Integrating climate trends with household resilience

6.1. Climate-driven intensification scenario

If erosivity increase is found in areas classified as high/severe under the 2024 RUSLE analysis, this would provide strong evidence that the climate-induced erosivity increase acts as an independent driver of erosion in the Beas Valley.

6.2. Adaptation-benchmarking scenario

Where erosion trends are significant but household clusters show intensive traditional-conservation practice, this signifies adaptive synergy, termed an "adaptive zone."

6.3. *Policy-priority scenario*

Areas exhibiting high erosivity trends and low conservation adoption, the "concordant zones" of Figure 2 and Table 5 (high erosivity trend co-occurring with low household adaptation), constitute the priority map for urgent conservation planning.

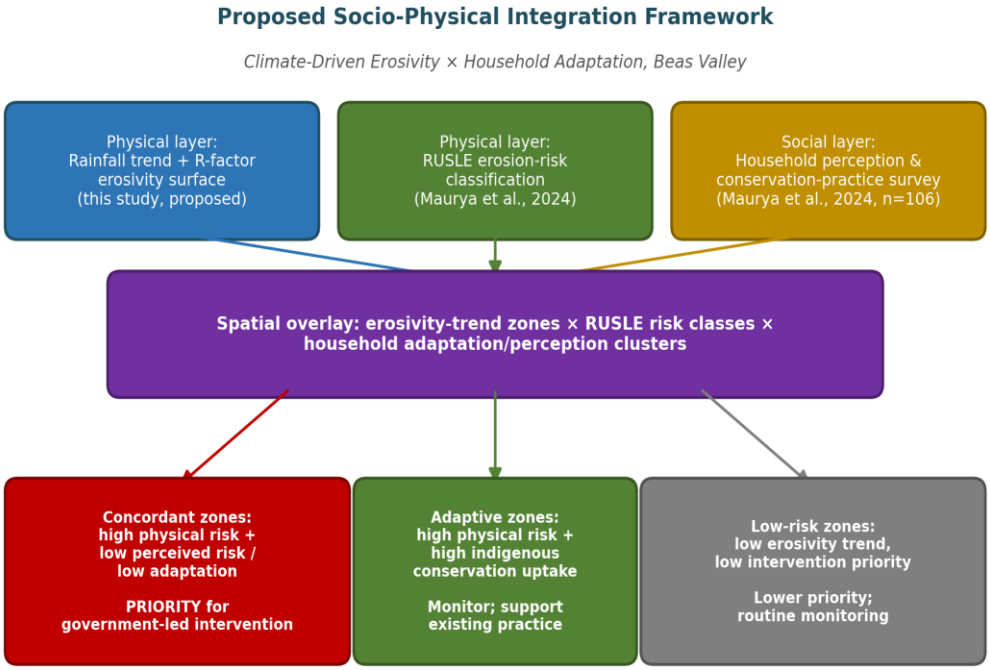

Figure 2. Proposed socio-physical integration framework combining the physical erosivity-trend and RUSLE risk layers (this study; [9]) with the household adaptation layer ([10]).

Table 5. Proposed Three-Way Zonal Classification Framework.

Zone type	Physical erosivity trend	Household adaptation	Recommended action
Concordant high-priority	High / rising	Low	Immediate government-led conservation intervention
Adaptive	High / rising	High (indigenous conservation active)	Monitor; support and reinforce existing practice
Lower priority	Low / stable	Any	Routine monitoring

6.4. *Human-environment feedback*

The framework treats the published perception-practice finding of [10] as the starting evidence motivating spatial integration, with Sections 6.1–6.3 adding the mechanism for locating and prioritizing that gap.

7. Expected contributions and policy relevance

This framework is designed to produce the first climate-linked, socially-integrated extension of the Beas Valley erosion-risk map, giving policymakers a single, spatially explicit priority map for allocating limited conservation resources. As set out in Section 3.2.1, prior basin-scale RUSLE applications (Alaknanda, Uttarakhand, Sutlej, Koshi) each stop at a physical priority map; this framework's contribution is the explicit overlay of household conservation behavior, separating "high physical risk" from "high physical risk with low adaptive capacity."

8. Conclusions

In this study, we set out to close two gaps in Beas Valley erosion research (the missing link between rainfall trends and modelled erosion risk, and the missing validation of physical risk against local perception) and obtain three concrete outcomes. First, compiling the real evidence base for this basin (Sections 3.1.1, 3.3) shows that the physical risk picture is not uniform: For agriculture and vegetation, the land covers most exposed to rainfall-erosivity dynamics carry the largest combined share of the moderate-to-very-high soil-loss-potential area in the basin (Table 2), while the only station-level rainfall record for this exact corridor found no significant trend through 2009 [14], meaning the widely assumed climate-erosion link has not, in fact, been demonstrated for this basin, only inferred from wider regional studies. Second, the worked example (Section 5.3) demonstrates that the three-way classification genuinely discriminates: It is architecturally capable of separating zones of high physical risk with low adaptation (immediate intervention priority) from zones where indigenous practice buffers that risk (monitoring priority), a distinction that, critically, neither the RUSLE map [9] nor the household survey (Section 3.4) can produce on its own. Third, the framework (the trend-detection protocol, the product-selection rules, and the zonal-integration procedure, Section 4) is specified and reproducible, and is therefore usable immediately by this or any research team with access to gridded rainfall data for a Himalayan basin.

The concrete path forward is basin-wide execution, and it is specific rather than open-ended: (i) acquire the IMD 0.25° gridded daily rainfall record (or CHIRPS/CMORPH per Section 4.1) for 1990–2020; (ii) run the Mann-Kendall/Sen's-slope trend test and MFI/EI_{30} erosivity estimation specified in Sections 4.3–4.4.1; (iii) execute the zonal-statistics overlay of Section 4.6 against the real RUSLE classes of Table 2 and the household adaptation index of Section 4.5 to produce an actual, non-illustrative Table 4 and the spatio-temporal trend map; and (iv) validate the resulting priority zones against field-identified erosion features (Section 4.6.2) before handing the output to Kullu District and Himachal Pradesh soil- and water-conservation authorities as the basis for resource allocation.

Beyond the Beas Valley, the framework's replicability (Section 4.7) makes it directly transferable to other Himalayan basins where a physical erosion model and household adaptation survey exist independently but have not been spatially integrated, a combination that, per the literature reviewed in Section 3.2.1, is common across the region.

9. Limitations and future directions

Outputs reflect the quality of input layers; the household survey is a single cross-sectional snapshot; the three data layers span different time windows; coarse rainfall-grid resolution is addressed via micro-watershed integration and orographic downscaling (4.6.1); and gridded-product uncertainty is bounded via the sensitivity analysis (4.6.2). These considerations define the conditions under which the framework's outputs are most robust rather than restricting its applicability.

This paper's scope is a fully specified, replicable methodological framework, grounded in real evidence and demonstrated via a worked illustrative example (Section 5.3), rather than a basin-wide empirical results paper. Basin-wide execution (computing actual trend and erosivity values on a full multi-decadal gridded rainfall record, and the accompanying sensitivity and validation analyses) is explicitly identified as the framework's immediate next application rather than a gap in this paper's scope. The specific zone assignments, trend magnitudes, and priority rankings in Section 5.3's worked example illustrate the framework's mechanics and should not be cited as empirical findings for the Beas Valley.

Author contributions

Suraj Kumar Maurya: Conceptualization, Methodology, Formal analysis, Investigation, Writing–original draft; Vartika Singh: Data curation, Investigation, Writing–review & editing; Sujay Sarkar: Methodology, Validation, Writing–review & editing; Prabuddh Kumar Mishra: Supervision, Writing–review & editing. All authors have read and agreed to the published version of the manuscript.

Data availability statement

As this paper's scope is a methodological framework specification (Section 1), no basin-wide rainfall/erosivity dataset was generated for this submission. The RUSLE erosion-risk classification and household survey data referenced in Sections 3.3–3.4 are published in [9] and [10] respectively, and Table 2 reproduces the former's published results directly. Table 4 (Section 5.3) presents a worked illustrative example, not a basin-wide dataset. Upon basin-wide execution of the framework (identified in Section 9 as the immediate next application), the underlying gridded rainfall data, processing scripts, and computed trend/erosivity outputs will be made available in a publicly accessible repository to support replication.

Use of AI tools declaration

The authors declare they have not used Artificial Intelligence (AI) tools in the creation of this article.

Acknowledgments

This research received no specific grant from any funding agency in the public, commercial, or not-for-profit sectors. The authors gratefully acknowledge the India Meteorological Department (IMD)

and the developers of the CHIRPS and CMORPH gridded rainfall products for making their datasets openly available.

Conflict of interest

All authors declare no conflicts of interest in this paper.

References

1. Renard KG, Foster GR, Weesies GA, et al. (1997) Predicting Soil Erosion by Water: A Guide to Conservation Planning With the Revised Universal Soil Loss Equation (RUSLE). USDA Agriculture Handbook No. 703. Available from: https://www.ars.usda.gov/ARSUserFiles/60600505/RUSLE/AH_703%20-%20Predicting%20Soil%20Erosion%20by%20Water%20-%20A%20Guide%20to%20Conservation%20Planning%20With%20the%20RUSLE%20(RUSLE).pdf.
2. Wischmeier WH, Smith DD (1978) Predicting Rainfall Erosion Losses. USDA Agriculture Handbook No. 537. Available from: https://www.ars.usda.gov/ARSUserFiles/60600505/RUSLE/AH_537%20Predicting%20Rainfall%20Soil%20Losses.pdf.
3. Kumar A, Attri PK (2024) Analysis of pre-monsoon and post-monsoon seasonal rainfall trends by Mann-Kendall and Sen's slope estimator test in Himachal Pradesh, India. *Curr World Environ* 19: 998–1010. http://dx.doi.org/10.12944/CWE.19.2.37
4. Kumar P, Deka D, Husain MA, et al. (2025) Trend analysis of precipitation and temperature in Lahaul-Spiti district, Himachal Pradesh, India. *Front Clim* 6: 1348132. https://doi.org/10.3389/fclim.2024.1348132
5. Kumar P, Sarda R, Thakur S, et al. (2026) Investigating long term rainfall trends (1901–2021) and forecast over the mountainous state of India using machine learning approach. *Singapore J Trop Geo*. https://doi.org/10.1111/sjtg.70054
6. Manzoor S, Ahmad Ahanger M (2022) Spatio-temporal trends in precipitation and temperature means/extremes in the Himalayan states of India. *J Water Clim Change* 13: 2531–2558. https://doi.org/10.2166/wcc.2022.395
7. Kumar A, Devi M, Deshmukh B (2014) Integrated Remote Sensing and Geographic Information System Based RUSLE Modelling for Estimation of Soil Loss in Western Himalaya, India. *Water Resour Manage* 28: 3307–3317. https://doi.org/10.1007/s11269-014-0680-5
8. Gupta S, Kumar S (2017) Simulating climate change impact on soil erosion using RUSLE model: A case study in a watershed of mid-Himalayan landscape. *J Earth Syst Sci* 126: 43. https://doi.org/10.1007/s12040-017-0823-1
9. Maurya SK, Singh V, Chand K, et al. (2024) Assessment of soil erosion in the Beas Valley, Kullu, Himachal Pradesh. *Soil Sci Ann* 75: 185558. https://doi.org/10.37501/soilsa/185558
10. Maurya SK, Singh V, Chand K, et al. (2024) Perceptions and practices of indigenous soil conservation measures in Beas Valley. *GeoJournal* 89: 87. https://doi.org/10.1007/s10708-024-11068-9

11. Sharma A, Sajjad H, Saha TK, et al. (2024) Analyzing trend and forecasting of temperature and rainfall in Shimla district of Himachal Pradesh, India using non-parametric and bagging REPTree machine learning approaches. *J Atmos Sol-Terr Phy* 265: 106352. https://doi.org/10.1016/j.jastp.2024.106352
12. Das S, Jain MK, Auerswald K, et al. (2025) Identifying monthly rainfall erosivity patterns using hourly rainfall data across India. *Sci Rep* 15: 27940. https://doi.org/10.1038/s41598-025-11992-x
13. Mondal PP, Zhang Y (2018) Research progress on changes in land use and land cover in the Western Himalayas (India) and effects on ecosystem services. *Sustainability* 10: 4504. https://doi.org/10.3390/su10124504
14. Jangra S, Singh M (2011) Analysis of rainfall and temperatures for climatic trend in Kullu valley. *MAUSAM* 62: 77–84.
15. Singh S, Kansal ML (2024) Sub-basin prioritisation using RUSLE in a mountainous river basin of Uttarakhand. *Environ Dev Sustain* 26: 6851–6877. https://doi.org/10.1007/s10668-023-02989-5
16. George J, Kumar S, Hole RM (2021) Geospatial modelling of soil erosion and risk assessment in the Indian Himalayan region: A study of Uttarakhand state. *Environ Adv* 4: 100039. https://doi.org/10.1016/j.envadv.2021.100039
17. Sharma N, Kaushal A, Yousuf A, et al. (2022) Geospatial technology for assessment of soil erosion and prioritization of watersheds using RUSLE model for lower Sutlej sub-basin of Punjab, India. *Environ Sci Pollut Res* 30: 515–531. https://doi.org/10.1007/s11356-022-22152-3
18. Sharma N, Kaushal A, Yousuf A, et al. (2024) Prioritization of sub-watersheds and subsequent site identification for soil water and conservation practices using the SWAT-AHP integrated model in the Lower Sutlej Sub-basin, India. *Environ Sci Pollut Res* 31: 23120–23145. https://doi.org/10.1007/s11356-024-32382-2
19. Uddin K, Murthy MSR, Wahid SM, et al. (2016) Estimation of soil erosion dynamics in the Koshi basin using GIS and remote sensing to assess priority areas for conservation. *PLOS One* 11: e0150494. https://doi.org/10.1371/journal.pone.0150494
20. Taloor AK, Khajuria V, Parsad G, et al. (2025) Geospatial assessment of soil erosion in the Basantar and Devak watersheds of the NW Himalaya: A study utilizing USLE and RUSLE models. *Geosyst Geoenvironment* 4: 100355. https://doi.org/10.1016/j.geogeo.2025.100355
21. Prashanth M, Kumar A, Dhar S, et al. (2023) Land use/land cover change and its implication on soil erosion in an ecologically sensitive Himachal Himalayan watershed, Northern India. *Front For Glob Change* 6: 1124677. https://doi.org/10.3389/ffgc.2023.1124677
22. Dogra A, Thakur J, Tandon A (2023) Do satellite-based products suffice for rainfall observations over data-sparse complex terrains? *Remote Sens Environ* 299: 113855. https://doi.org/10.1016/j.rse.2023.113855
23. Upadhyaya A, Rai AK, Kumar P (2023) Anomalous rainfall trends in the North-Western Indian Himalayan Region (NW-IHR). *Theor Appl Climatol* 151: 253–272. https://doi.org/10.1007/s00704-022-04280-5
24. Prakash S (2019) Performance assessment of CHIRPS, MSWEP, SM2RAIN-CCI, and TMPA precipitation products across India. *J Hydrol* 571: 50–59. https://doi.org/10.1016/j.jhydrol.2019.01.036

25. Banerjee A, Chen R, Meadows ME, et al. (2020) An analysis of long-term rainfall trends and variability in the Uttarakhand Himalaya using Google Earth Engine. *Remote Sens* 12: 709. https://doi.org/10.3390/rs12040709
26. Mondal S, Jeganathan C (2022) Effect of scale, landscape heterogeneity and terrain complexity on agriculture mapping accuracy from time-series NDVI in the Western-Himalaya region. *Landsc Ecol* 37: 2757–2781. https://doi.org/10.1007/s10980-022-01533-6
27. Pandey K, Kumar S, Sekar KC (2026) Farmer perceptions of climate variability, adaptation practices, and livelihood implications in the Garhwal Himalaya. *Discov Sustain* 7: 760. https://doi.org/10.1007/s43621-026-03502-4
28. Namgyal P, Sarkar S, Kumar R (2025) Vulnerability assessment of rural households to climate change using livelihood vulnerability framework approach in the trans-Himalayan region of Ladakh, India. *Anthropocene* 49: 100467. https://doi.org/10.1016/j.ancene.2025.100467
29. Mann HB (1945) Nonparametric tests against trend. *Econometrica* 13: 245–259.
30. Kendall MG (1975) *Rank Correlation Methods*, 4th ed., Charles Griffin, London.
31. Sen PK (1968) Estimates of the regression coefficient based on Kendall's tau. *J Am Stat Assoc* 63: 1379–1389. https://doi.org/10.1080/01621459.1968.10480934
32. Benjamini Y, Hochberg Y (1995) Controlling the false discovery rate: A Practical and Powerful Approach to Multiple Testing. *J R Stat Soc B* 57: 289–300. https://doi.org/10.1111/j.2517-6161.1995.tb02031.x
33. Yue S, Pilon P, Phinney B, et al. (2002) The influence of autocorrelation on the ability to detect trend in hydrological series. *Hydrol Process* 16: 1807–1829. https://doi.org/10.1002/hyp.1095
34. Hamed KH, Rao AR (1998) A modified Mann-Kendall trend test for autocorrelated data. *J Hydrol* 204: 182–196. https://doi.org/10.1016/S0022-1694(97)00125-X
35. Bhatnagar S, Chaudhary R, Janjhua Y, et al. (2026) Mitigating livelihood vulnerability of farm households through climate-smart agriculture in North-Western Himalayan region. *Resources* 15: 14. https://doi.org/10.3390/resources15010014
36. Golijanin J, Nikolić G, Valjarević A, et al. (2022) Estimation of potential soil erosion reduction using GIS-based RUSLE under different land cover management models: A case study of pale municipality, B&H. *Front Environ Sci* 10: 945789. https://doi.org/10.3389/fenvs.2022.945789



AIMS Press

© 2026 the Author(s), licensee AIMS Press. This is an open access article distributed under the terms of the Creative Commons Attribution License (https://creativecommons.org/licenses/by/4.0)